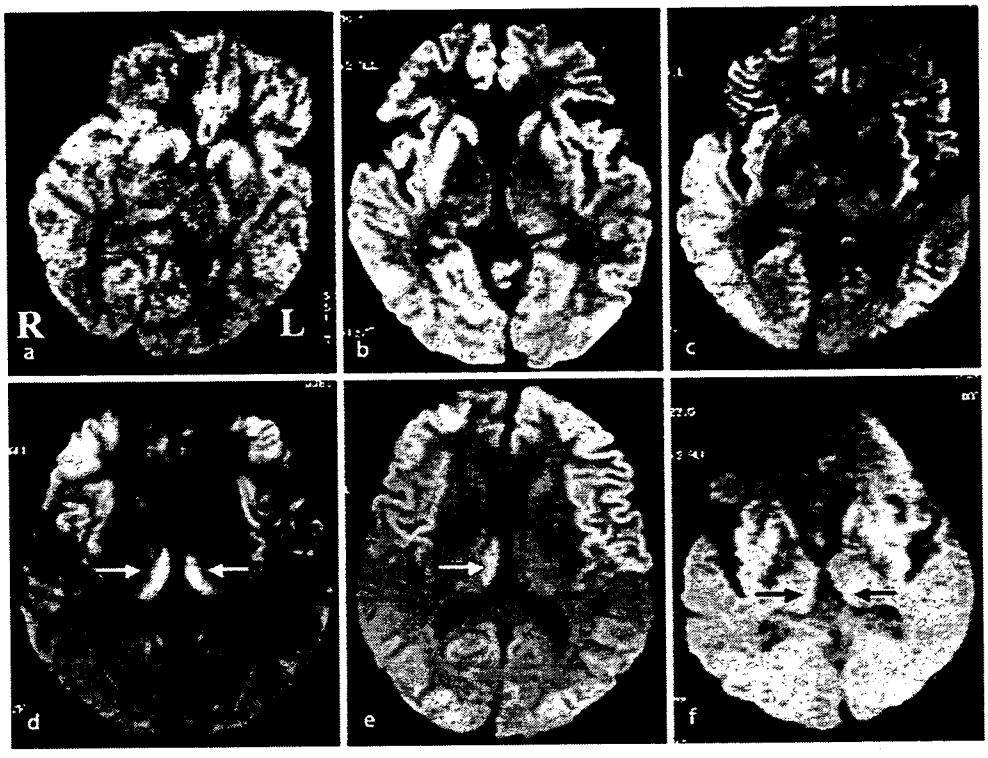

Fig. 3 DWI of the rapid-type group (**A–C**) and the slow-type group (**D–F**). **A** DWI obtained from a 55-year-old woman demonstrating high-intensity lesions mainly in the bilateral striatum. The right temporal cortex demonstrated slightly high-intensity lesions. **B** DWI obtained from a 60-year-old woman demonstrating high intensity lesions in the frontal, temporal, occipital and insular cortex, and the striatum. The right side predominated. **C** DWI obtained from a 62-year-old woman demonstrating high-intensity lesions in the bilateral occipital and insular cortex. The right temporal cortex was also depicted as an area of high intensity. We did not find high-intensity lesions in the striatum. **D** DWI obtained from a 69-year-old woman demonstrating high-intensity lesions in the bilateral frontal and insular cortex. The bilateral caudate head showed slightly high-intensity lesions. Interestingly, the bilateral medial thalami showed high-intensity lesions with the so-called hockey stick sign (white arrows). **E** DWI obtained from a 70-year-old man demonstrating high-intensity lesions in the bilateral frontal, occipital, and insular cortex. The right medial thalamus also showed high intensity (white arrow). **F** DWI obtained from a 52-year-old man demonstrating high-intensity lesions in the right temporal cortex and the left striatum. The bilateral medial thalami also showed high intensity lesion (black arrows)

no family history of prion disease had the M232R substitution: one was previously reported, pathologically confirmed dementia with Lewy bodies [12], one was encephalitis, and one was not diagnosed yet, but was confirmed as not having CJD because his symptoms rather fluctuated. There remains the possibility that the M232R substitution is a rare polymorphism, not a causative point mutation [6], although the M232R substitution was not found among 100 healthy controls [4].

Discussion

In the present study, by reviewing the clinical and laboratory findings of 21 patients, we found that there were two distinct phenotypes in CJD232 in spite of the same genotype of PRNP, M232R, MM129, and GG219. Different phenotypes with the same pathogenic changes of PRNP are known in several types of genetic prion disease [14–21]. Fatal familial insomnia and gCJD with a common point mutation at codon 178 are well-known. However, the different phenotypes are regulated by a polymorphism at codon 129 [14, 15]. Similarly, a phenotypic variant of gCJD with a point mutation of glutamic acid to lysine at codon 200 (CJD200) is coupled with valine at codon 129 [19]. On the other hand, a thalamic variant of CJD200, which has the same polymorphism of MM129 as the vast majority of CJD200, has been reported [17, 21], although it is exceptional. In our results, 15 of the patients were the rapid-type, five were the slow-type. In CJD232, the slow-type, which has uncommon clinical features, is not exceptional and constitutes one of the major phenotypes because 25% of patients with CJD232 belong to the slow-type. Similarly, there are two different major phenotypes that are not influenced by the polymorphism of codon 129 and 219 in Gerstmann-Sträussler-Scherinker disease with a point mutation of proline to leucine at codon 102 of PRNP (GSS102), which is characterized by chronic cerebellar ataxia of long duration (several years or more) associated with neurological signs including dementia [21]. In GSS102, a sCJD-like variant of short duration (less than one year) has been reported [16]. In 27 patients with GSS102 recognized by the Creutzfeldt-Jakob Disease Surveillance

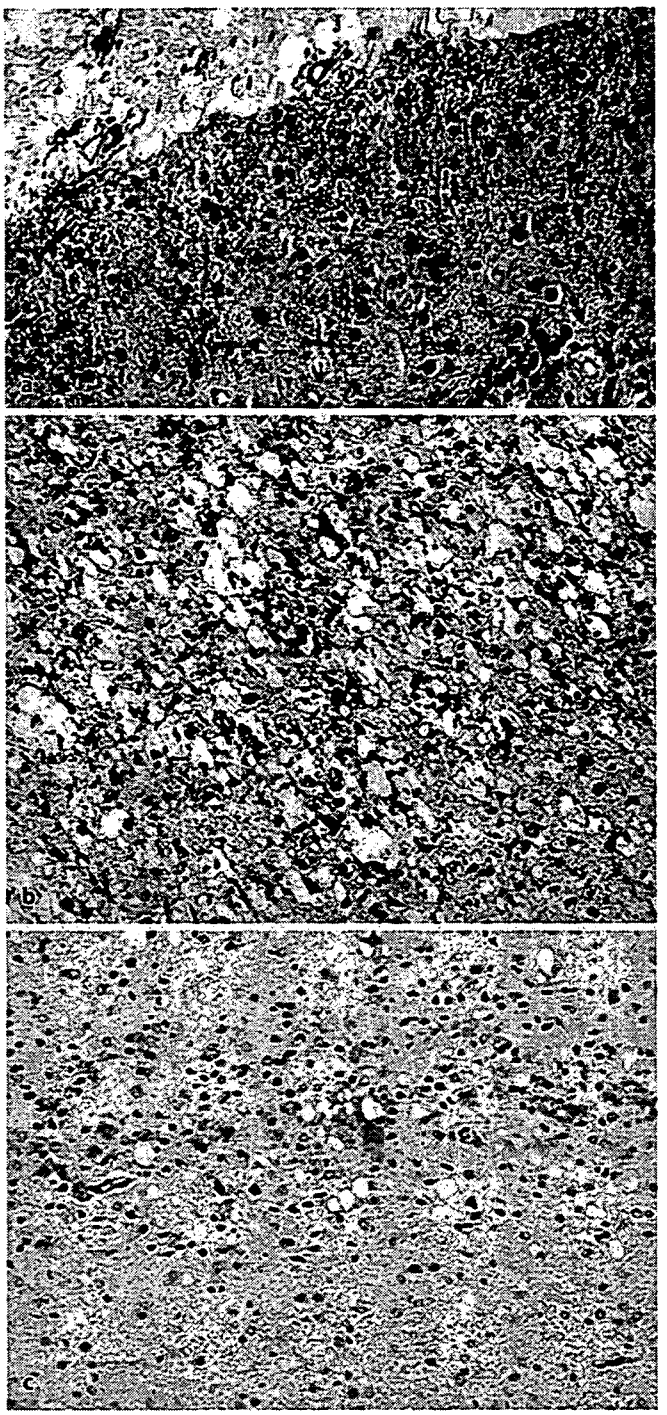

Fig. 4 Immunohistochemical staining of abnormal PrP using monoclonal antibody 3F4. **A** Anti-PrP immunostaining in a 67-year-old woman suffering from the rapid-type of CJD232 with an initial symptom of cerebellar ataxia. The molecular layer of the cerebellum shows a diffuse synaptic-type PrP deposit. Photographed at 200 times magnification. **B** Anti-PrP immunostaining in a 64-year-old woman suffering from the slow-type of CJD 232 with an initial symptom of dressing apraxia. This patient was previously reported by Satoh et al. (1997). The perivacuolar-type PrP deposit is predominantly demonstrated in the temporal cerebral cortex. Photographed at 50 times magnification. **C** Anti-PrP immunostaining in the same patient with Fig. 4B. The synaptic-type PrP deposit is demonstrated in the occipital cerebral cortex. Photographed at 50 times magnification

Committee, Japan until February 2006, five (18.5%) were this sCJD-like variant. It should be emphasized that CJD232 has two major different phenotypes with the completely same genotype of PRNP that is undoubtedly a major factor which influences the clinical phenotype [2, 22–24].

The gender and age at onset influence the disease progression [25]. However, there were no significant differences in the male to female ratio and age at onset between the two types in our series of CJD232. The molecular type of PrP^{Sc} is another factor that is closely associated with the clinical and pathological phenotypes of sCJD [26]. Unfortunately, the molecular type of PrP^{Sc} has not been sufficiently examined. One previously reported patient [27] in the rapid-type group had type 1 and one patient in the slow-type group had type 1 + 2. This difference may be a determinant of the clinical phenotypes of CJD232. More studies are needed to determine the relationship between the clinical phenotype and the molecular type of PrP^{Sc}. Immunohistochemical staining of PrP from four patients with the rapid-type revealed a diffuse synaptic-type deposit similar to that found in sCJD with MMI [28]. The synaptic-type PrP deposit may be an important pathological finding of the rapid-type. If so, we cannot differentiate the rapid-type of CJD232 from sCJD with MM1 based on the pathological findings. PrP immunohistochemical staining of three patients with the slow-type revealed that two had a perivacuolar-type and diffuse synaptic-type PrP deposits and one had only diffuse synaptic-type deposits. These pathological results suggest that the rapid-type might be a homogeneous group and the slow-type might not be. The number of studied patients in the two groups was too small to determine the pattern. If the PrP^{Sc} type 1 + 2 and the perivacuolar-type PrP deposits are key pathological features of the slow-type of CJD232, these may be related to the absence or late occurrence of myoclonus and PSWC on EEG, and the slower progression of the disease.

Diagnosing the rapid-type of CJD232 is not difficult because the patients start with progressing dementia, cerebellar ataxia, and visual problems, rapidly progress to akinetic mutism, demonstrate PSWC, are positive for 14-3-3 protein in the CSF immunoassay, and have characteristic MRI findings. These clinical features including the MRI findings are very similar to those of typical sCJD with MM1 [3] that accounts for the vast majority of sCJD. We can easily suspect CJD when we encounter such patients. Genetic examination of PRNP is necessary to differentiate the rapid-type of CJD232 from sCJD with MM1 [3] since a patient with CJD232 usually has no family history of prion disease or dementia, and differentiating CJD232 from sCJD with MM1 [3] is difficult when based on the clinical and laboratory features alone.

On the other hand, diagnosing the slow-type of

Table 1 Comparison of clinical and laboratory features between the rapid-type (R-type) and the slow-type (S-type) of CJD232

Clinical features	R-type (N = 15)	S-type (N = 5)	p
Age at onset (Year)	65.4 ± 5.2	59.0 ± 12.8	NS
Men: Women	8: 7	2: 3	NS
Family history	0/15 positive	0/5 positive	NS
Initial symptoms	7: progressive dementia 2: visual symptoms 2: cerebellar ataxia 2: involuntary movement 2: others	3: progressive dementia 1: psychiatric symptoms 1: dressing apraxia	
Myoclonus (Mo)[a]	2.4 ± 1.8	15.3 ± 12.3	< 0.005
Positive rate	14/14[b]	4/5*	NS
Akinetic mutism (Mo)[a]	3.1 ± 1.5	20.6 ± 4.4	< 0.001
Positive rate	15/15	5/5	NS
14-3-3 protein	8/8 positive	4/4 positive	NS
PSWC (Mo)[a]	2.8 ± 1.8	13	< 0.01
Positive rate	15/15	1/5**	< 0.01
MRI	8/9 positive	4/5 positive	NS
Codon 129	15: Met/Met	5: Met/Met	
Codon 219	14: Glu/Glu 1: Glu/Lys	5: Glu/Glu	
Autopsied cases	5/15	3/5	
PrP immunostaining	Synaptic 4	Synaptic + Perivacuolar 2 Synaptic 1	
PrP type	Type 1: 1	Type 1 + 2: 1	

Values are means ± SD where applicable

[a] The duration until the appearance of myoclonus, akinetic mutism, and PSWC from the onset; [b] It was uncertain whether myoclonus had appeared or not in one patient

* Mean observation period was 14.8 ± 10.7 months; ** Mean observation period was 21.6 ± 12.8 months

R-type the rapid-type of CJD232; *S-type* the slow-type of CJD232; *PSWC* periodic sharp and wave complexes in EEG; *PRNP* prion protein gene; *Met/Met* methionine homozygosity; *Glu/Glu* glutamic acid homozygosity; *Glu/Lys* heterozygosity of glutamic acid and lysine; *NS* not significant

CJD232 is not easy because the patients initially manifest non-characteristic dementia or memory disturbance, or psychiatric symptoms as in other neurodegenerative disorders, progress relatively slowly, do not become akinetic and mute within a year, and do not demonstrate PSWC. When we diagnose the slow-type of CJD232, we cannot rely on PSWC, the presence of which is the most widely accepted diagnostic marker at the present time. In addition to the slow progression, the lack of a family history may cause this disease to be confused with other neurodegenerative disorders such as Alzheimer's disease, dementia with Lewy bodies, corticobasal degeneration, frontotemporal dementia, etc., especially in the early phase. MRI, especially DWI [11], is very useful to distinguish the slow-type of CJD232 from other neurodegenerative disorders, because the slow-type of CJD232 demonstrates CJD-related high-intensity lesions in DWI, whereas the above-mentioned neurodegenerative disorders do not demonstrate abnormal changes in signal intensities. There has been a report of suspected CJD patients who had M232R and in whom a final pathological diagnosis of dementia with Lewy bodies demonstrated no signal changes in DWI [12]. In our series of three patients with the slow-type examined by DWI, medial thalamic lesions were demonstrated. However, these lesions are not specific for the slow-type of CJD232, and we sometimes encounter them in sCJD [29]. The major differential diagnosis of the slow-type of CJD232 is sCJD with the MM2-cortical type [3], because the slow-type of CJD232 usually fulfills the previously advocated diagnostic criteria for sCJD with the MM2 cortical type [30]. It is hardly possible clinically to distinguish the slow-type of CJD232 from sCJD with the MM2 cortical type. However, the molecular type of PrP^{Sc} in one patient of the slow-type CJD232 was type 1 + 2, not type 2. The molecular types of PrP^{Sc} in each group may be different, although the presence of perivacuolar-type PrP deposits is also a finding of sCJD with the MM2-cortical type [3]. PRNP study is indispensable to distinguish between the two groups and molecular typing may be able to distinguish between them. We did not find any peculiar lesions of the slow-type such as a remarkable high intensity lesion in the cerebral cortex except for those in the medial occipital and cerebellar cortices which are characteristic of fCJD with a point mutation of valine to isoleucine at codon 180 (CJD180),

which is an unusual type of fCJD [13]. The degree of the abnormalities in MRI did not correlate with the disease severity. To diagnose the slow type of CJD232, recognizing the clinical phenotype that demonstrates uncommon clinical and laboratory features found in other neurodegenerative disorders with dementia and performing genetic examination of PRNP are important.

Other characteristics of CJD232 are that CJD232 patients have no family history of CJD or dementia in either type and are reported only in Japan. More than half of genetic prion disease patients with various PRNP mutations lack family histories and the lack of family histories is not restricted to CJD232 [1]. De novo mutations [31] and very low penetration [32] are considered as the reasons. Individual PRNP mutations also show variable geographical distributions [1]. The M232R substitution may influence the disease progression because the M232R substitution extended the incubation time in an experimental transmission study using humanized knock-in mice [33]. Three suspected patients with M232R substitution but with a final diagnosis of diseases other than CJD have been reported to the Creutzfeldt-Jakob Disease Surveillance Committee, Japan because they had the M232R substitution, not because they had clinical symptoms suspecting CJD. Therefore, we think that the prevalence of 6 % in 50 non-CJD patients is not the same as that of the normal Japanese population. At least, it cannot be said that all patients having the M232R substitution demonstrate the symptoms of CJD232, and it does not seem to be supported that M232R substitution is a causative mutation. On the other hand, two probable CJD patients with M232R substitution in one family have been reported [6]. We cannot overlook these patients based on the fact that M232R substitution is very rare [4]. Whether M232R is really a causative mutation or only a rare polymorphism is another issue that needs to be resolved. We need more studies of CJD patients with M232R substitution, and especially the correlation between the pathological findings including the molecular type of PrP^{Sc} and immunohistochemical staining of PrP and the clinical findings should be clarified to determine whether it influences the disease progression. We need to study the morbidity of a population having the M232R substitution to determine whether it is a causative mutation or not.

Acknowledgement We thank Mr. Brent Bell for reading the manuscript. We also wish to thank all the doctors for their care of the patients. This study was based on the fruits of the Creutzfeldt-Jakob Disease Surveillance Committee, Japan and was supported in part by a grant from the Research Committee on Prion Disease and Slow Virus Infection, Ministry of Labor and Health, Japan. Yusei Shiga, Tetsuyuki Kitamoto, Shigetoshi Kuroda, Takeshi Sato, Yoshikazu Nakamura, Masahito Yamada, and Hidehiro Mizusawa are the members of the Creutzfeldt-Jakob Disease Surveillance Committee, Japan. The surveillance study of the Creutzfeldt-Jakob Disease Surveillance Committee, Japan was approved by the ethics committee of Kanazawa University.

References

1. Kovács GG, Puopolo M, Ladogana A, et al. (2005) Genetic prion disease: the EUROCJD experience. Hum Genet 118:166–174
2. Kovács GG, Trabattoni G, Heinfellner JA, Ironside JW, Knight RSG, Budka H (2002) Mutations of the prion protein gene: Phenotypic spectrum. J Neurol 249:1567–1582
3. Parchi P, Giese A, Capellari S, et al. (1999) Classification of sporadic Creutzfeldt-Jakob disease based on molecular and phenotypic analysis of 300 subjects. Ann Neurol 46:224–233
4. Kitamoto T, Ohta M, Doh-ura K, Hitoshi S, Terao Y, Tateishi J (1993) Novel missense variants of prion protein in Creutzfeldt-Jakob disease or Gerstmann-Sträussler Syndrome. Biochem Biophys Res Commun 191:709–714
5. Shimizu T, Tanaka K, Tanahashi N, Fukuuchi Y, Kitamoto T (1994) Creutzfeldt-Jakob disease with a point mutation at codon 232 of prion protein – A case report. Clin Neurol 34: 590–592
6. Hoque MZ, Kitamoto T, Furukawa H, et al. (1996) Mutation in the prion protein gene at codon 232 in Japanese patients with Creutzfeldt-Jakob disease: a clinicopathological, immunohistochemical and transmission study. Acta Neuropathol 92:441–446
7. Satoh A, Goto H, Satoh H, et al. (1997) A case of Creutzfeldt-Jakob disease with a point mutation at codon 232: Correlation of MRI and neurological findings. Neurology 49:1469–1470
8. Saito T, Isozumi K, Komatsumoto S, Nara M, Suzuki K, Doh-ura K (2000) A case of codon 232 mutation-induced Creutzfeldt-Jakob disease visualized by the MRI-FLAIR images with atypical clinical symptoms. Clin Neurol 40: 51–54
9. Tagawa A, Natsuno T, Suzuki M, Ono S, Shimizu N (2001) Creutzfeldt-Jakob disease with codon 232 point mutation and showing myoclonus and PSD in the early stage. A case report. Neurol Med 54:161–165
10. Hitoshi S, Nagura H, Yamanouchi H, Kitamoto T (1993) Double mutations at codon 180 and codon 232 of the PRNP gene in an apparently sporadic case of Creutzfeldt-Jakob disease. J Neurol Sci 120:208–212
11. Shiga Y, Miyazawa K, Sato S, et al. (2004) Diffusion-weighted MRI abnormalities as an early diagnostic marker for Creutzfeldt-Jakob disease. Neurology 63:443–449
12. Koide T, Ohtake H, Nakajima T, et al. (2002) A patient with dementia with Lewy bodies and codon 232 mutation of PRNP. Neurology 59:1619–1621
13. Jin K, Shiga Y, Shibuya S, et al. (2004) Clinical features of Creutzfeldt-Jakob disease with V180I mutation. Neurology 62:502–505
14. Goldfarb LG, Peterson RB, Tabaton M, et al. (1992) Fatal familial insomnia and familial Creutzfeldt-Jakob disease: disease phenotype determined by a DNA polymorphism. Science 258: 806–808

15. Monari L, Chen SG, Brown P, et al. (1994) Fatal familial insomnia and familial Creutzfeldt-Jakob disease: different prion proteins determined by a DNA polymorphism. Proc Natl Acad Sci 91:2839–2842
16. Barbanti P, Fabbrini G, Salvatore M, et al. (1996) Polymorphism at codon 129 or 219 of PRNP and clinical heterogeneity in a previously unreported family with Gerstmann-Sträussler-Scherinker disease (PrP-P102L mutation). Neurology 47:734–741
17. Chapman J, Arlazoroff A, Goldfarb LG, et al. (1996) Fatal insomnia in a case of familial Creutzfeldt-Jakob disease with the codon 200^{Lys} mutation. Neurology 46:758–761
18. Young K, Clark HB, Piccardo P, Dlouhy SR, Ghetti B (1997) Gerstmann-Sträussler-Scherinker disease with the PRNP P102L mutation and valine at codon 129. Molecular Brain Research 44:147–150
19. Hainfellner JA, Parchi P, Kitamoto T, Jarius C, Gambetti P, Budka H (1999) A novel phenotype in familial Creutzfeldt-Jakob disease: Prion protein gene E200K mutation coupled with valine at codon 129 and type 2 protease-resistant prion protein. Ann Neurol 45:812–816
20. Yamada M, Itoh Y, Inaba A, et al. (1999) An inherited prion disease with a PrP P105L mutation: Clinicopathologic and PrP heterogeneity. Neurology 53: 181–188
21. Teratuto AL, Piccardo P, Reich EG, et al. (2002) Insomnia associated with thalamic involvement in E200K Creutzfeldt-Jakob disease. Neurology 58:362–267
22. Doh-ura K, Tateishi J, Sasaki H, Kitamoto T, Sasaki Y (1989) Pro-leu change at position 102 of prion protein is the most common but not the sole mutation related to Gerstmann-Sträussler syndrome. Biochem Biophys Res Commun 163:974–979
23. Furukawa H, Kitamoto T, Tanaka Y, Tateishi J (1995) New variant prion protein in a Japanese family with Gerstmann-Sträussler-Scherinker syndrome. Brain Res Mol Brain Res 30:385–388
24. Shibuya S, Higuchi J, Shin RW, Tateishi J, Kitamoto T (1998) Codon 219 Lys allele of PRNP is not found in sporadic Creutzfeldt-Jakob disease. Ann Neurol 43:826–828
25. Pocchiari M, Puopolo M, Croes EA, et al. (2004) Predictors of survival in sporadic Creutzfeldt-Jakob disease and other human transmissible spongiform encephalopathies. Brain 127: 2348–2359
26. Hill AF, Joiner S, Wadsworth JD, et al. (2003) Molecular classification of sporadic Creutzfeldt-Jakob disease. Brain 126:1333–1346
27. Satoh K, Muramoto T, Tanaka T, et al. (2003) Association of an 11–12 kDa protease-resistant prion protein fragment with subtypes of dura graft-associated Creutzfeldt-Jakob disease and other prion diseases. J General Virol 84:2885–2893
28. Kitamoto T, Shin RW, Doh-ura K, et al. (1992) Abnormal isoform of prion proteins accumulates in the synaptic structures of the central nervous system in patients with Creutzfeldt-Jakob disease. Am J Pathol 140:1285–1294
29. Young GS, Geschwind MD, Fischbein NJ, et al. (2005) Diffusion-weighted and fluid-attenuated inversion recovery imaging in Creutzfeldt-Jakob disease: High sensitivity and specificity for diagnosis. Am J Neuroradiol 26: 1551–1562
30. Hamaguchi T, Kitamoto T, Sato T, et al. (2005) Clinical diagnosis of MM2-type sporadic Creutzfeldt-Jakob disease. Neurology 64:643–648
31. Dagvadorj A, Peterson RB, Lee HS, et al. (2003) Spontaneous mutations in the prion protein gene causing transmissible spongiform encephalopathy. Ann Neurol 52:355–359
32. Mitrova E, Belay Gl (2002) Creutzfeldt-Jakob disease with E200K mutation in Slovakia: characterization and development. Acta Virol 46:31–39
33. Taguchi Y, Mohri S, Ironside JW, Muramoto T, Kitamoto T (2003) Humanized knock-in mice expressing chimeric prion protein showed varied susceptibility to different human prions. Am J Pathol 163:2585–2593

Clinical features and diagnosis of dura mater graft–associated Creutzfeldt–Jakob disease

M. Noguchi-Shinohara, MD
T. Hamaguchi, MD, PhD
T. Kitamoto, MD, PhD
T. Sato, MD, PhD
Y. Nakamura, MD, MPH, FFPH
H. Mizusawa, MD, PhD
M. Yamada, MD, PhD

Address correspondence and reprint requests to Professor Masahito Yamada, Department of Neurology and Neurobiology of Aging, Kanazawa University Graduate School of Medical Science, 13-1, Takara-machi, Kanazawa 920-8640, Japan
m-yamada@med.kanazawa-u.ac.jp

ABSTRACT Background: A subset of patients with dura mater graft-associated Creutzfeldt-Jakob disease (dCJD) demonstrates atypical clinical features and plaque formation in the brain (plaque type). **Objective:** To elucidate the frequency and clinical features of plaque type dCJD in comparison with the non-plaque type. **Methods:** We analyzed clinicopathologic findings of 66 patients who had been registered as having dCJD by the Creutzfeldt-Jakob Disease Surveillance Committee, Japan, between April 1999 and February 2006. **Results:** 1) Analysis of pathologically confirmed dCJD patients (n = 23) demonstrated plaque type dCJD in 11 patients (48%). In contrast to the non-plaque type with classic CJD features, the plaque type commonly presented with ataxic gait as an initial manifestation, relatively slow progression of neurologic symptoms, and no or late occurrence of periodic sharp-wave complexes (PSWCs) on EEG. MRI, especially diffusion-weighted images, and CSF 14-3-3 protein and neuron specific enolase (NSE) showed high diagnostic sensitivities for plaque as well as non-plaque types. 2) Analysis of clinically diagnosed dCJD patients (n = 34) demonstrated that 7 patients (21%) had atypical clinical features without PSWCs, probably corresponding to plaque type dCJD. **Conclusion:** The frequency of the plaque type in dura mater graft-associated Creutzfeldt-Jakob disease is apparently higher than previously recognized. For the clinical diagnosis of the plaque type dura mater graft-associated Creutzfeldt-Jakob disease, MRI and CSF markers would be useful, in addition to the core features, i.e., onset with ataxic gait disturbance, relatively slow progression, and no or late occurrence of periodic sharp-wave complexes on EEG. **NEUROLOGY 2007;69:360-367**

To date, the total number of iatrogenic Creutzfeldt–Jakob disease (iCJD) patients has reached 405.[1] One of the most frequent causes of iCJD is human cadaveric dura mater grafts. Since the first report of dura mater graft–associated CJD (dCJD) in 1988,[2] 196 cases have been recognized worldwide,[1] and more than 50% of patients with dCJD have been found in Japan.[1]

Most dCJD patients show subacute progression of neurologic manifestations which are almost identical with those of classic sporadic CJD (sCJD).[3,4] However, some dCJD patients were reported to present with atypical clinicopathologic features[3-9]; these patients are characterized clinically by relatively slow progression of neurologic manifestations and scarcity of PSWCs on EEG, and pathologically by no or slight brain atrophy and presence of amyloid plaques immunoreactive for prion protein (PrP), frequently described as florid plaques.[3-9] Some clinicopathologic features of atypical dCJD with plaque formation, termed the plaque type, are similar to those of variant CJD (vCJD).[10]

It remains unknown why some patients develop the plaque type, while others develop the non-plaque type. For both types, a codon 129 polymorphism in the PrP gene was homozygous for methionine, and Western blot analysis of protease-resistant PrP (PrP^{res}) demonstrated type 1 pattern[9] according to Parchi's classification.[11,12]

In this study, we analyzed dCJD patients registered by the CJD Surveillance Commit-

From the Department of Neurology and Neurobiology of Aging (M.N.-S., T.H., M.Y.), Kanazawa University Graduate School of Medical Science, Kanazawa; Department of Prion Protein Research, Division of CJD Science and Technology (T.K.), Tohoku University Graduate School of Medicine, Sendai; Department of Neurology (T.S.), Higashi-Yamato Hospital, Higashiyamato; Department of Public Health (Y.N.), Jichi Medical University, Shimotsuke; Department of Neurology and Neurological Science (H.M.), Graduate School, Tokyo Medical and Dental University, Tokyo; and the Creutzfeldt–Jakob Disease Surveillance Committee (T.K., T.S., Y.N., H.M., M.Y.), Japan.

Disclosure: The authors report no conflicts of interest.

Immunohistochemical findings of the frontal cortex with an anti-prion protein (PrP) monoclonal antibody, 3F4, from patients with plaque type dura mater graft-associated Creutzfeldt-Jakob disease (dCJD)[8] (A) and with non-plaque type dCJD[13] (B). Plaque type (A) and diffuse, synaptic type PrP deposits (B) are shown. Scale bar, 50 μm.

Figure Immunohistochemical findings of the frontal cortex

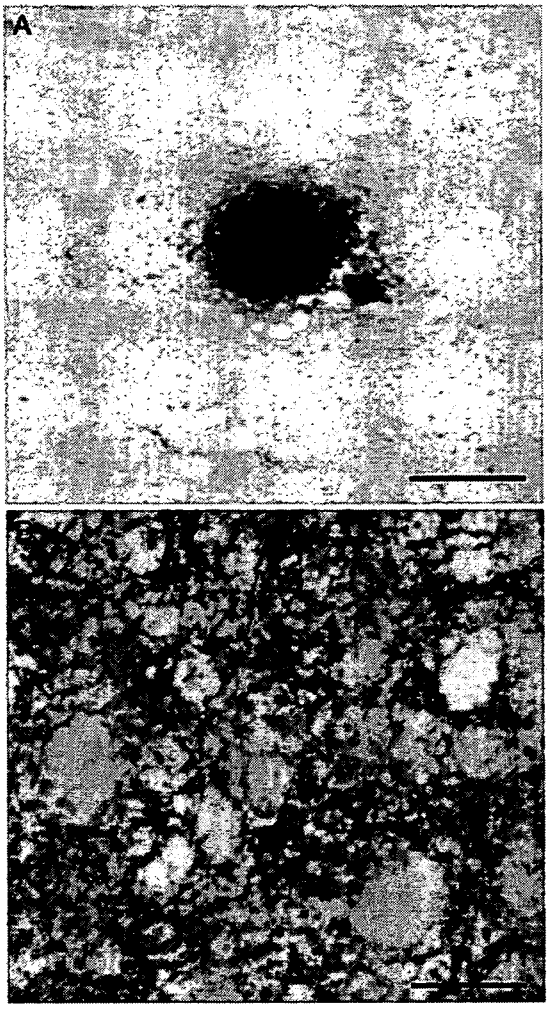

tee, Japan, to elucidate the frequency and clinical features of the plaque type compared with those of the non-plaque type.

METHODS Patients. We analyzed patients who had been prospectively registered as having prion diseases by the CJD Surveillance Committee, Japan, between April 1999 and February 2006. Under the surveillance system, each patient was investigated using a surveillance protocol including information about clinical history, neurologic findings, CSF markers, neuroimaging findings, molecular genetic analysis of PrP, and pathologic examinations.

We classified the patients into four categories: sCJD, environmentally acquired prion diseases, inherited prion diseases, and unclassified prion diseases. When CJD patients had a history of receiving cadaveric dura mater grafts during neurosurgical procedures, they were classified as dCJD patients, although we could not obtain any information on donors of the dura mater grafts. According to the neuropathologic findings obtained by the methods described below, dCJD patients with sufficient pathologic information were categorized into two types: the plaque type, which showed plaque type PrP deposits in the brain (figure, A),[8] and the non-plaque type, which showed synaptic type PrP deposits without obvious formation of PrP plaques (figure, B).[13]

Since the analysis of pathologically confirmed dCJD patients in our current study revealed that no patients with the plaque type showed PSWCs on EEG within 12 months after onset, and in contrast, all patients with the non-plaque type showed PSWCs within 5 months, we separated pathologically unconfirmed dCJD patients into a PSWCs positive (PSWCs[+]) group with PSWCs within 12 months and a PSWCs negative (PSWCs[−]) group with no PSWCs within 12 months. PSWCs(−) patients in whom the duration between onset and investigation was shorter than 12 months were excluded from this study because PSWCs may appear after the investigation. When clinical manifestations were analyzed for pathologically unconfirmed dCJD patients, only the patients who had been observed until death were included to assess manifestations throughout the entire clinical course.

Clinical and laboratory studies. For clinical and laboratory data, we analyzed the sex, site of dura mater graft, year of dura mater grafting, source of dura mater, age at dura mater grafting, incubation period between dura mater grafting and onset of CJD, age at onset of CJD, initial symptoms, neurologic manifestations during the entire clinical course, duration between onset of CJD and death, PSWCs on EEG, brain MRI findings, 14-3-3 protein and neuron specific enolase (NSE) in CSF, and PrP genotypes. For MRI, we evaluated high intensity lesions in the basal ganglia, thalamus, and cortical ribbons on diffusion-weighted images (DWI), fluid-attenuated inversion recovery (FLAIR) images, or T2-weighted images (T2WI). In addition, because DWI has been reported to be able to demonstrate early brain lesions of prion diseases even when scans are negative on FLAIR or T2WI,[14] we separately evaluated cases analyzed with DWI. The 14-3-3 protein immunoassay was performed by Western blot using polyclonal antibody SC629 (Santa Cruz Biotechnology, Santa Cruz, CA).[15] NSE in CSF was measured using a commercial ELISA kit as previously described.[15] For PrP gene analysis, DNA was extracted from blood, and the open reading frame of the PrP gene was analyzed as previously described.[16,17]

Neuropathology and Western blot analysis. Brain tissues obtained at autopsy were sectioned and stained by routine neuropathologic techniques. Immunohistochemistry was performed with a monoclonal antibody to PrP (3F4), as previously described.[16] Brain tissue was homogenized, and Western blot analysis of PrP^{res} was performed with 3F4 as previously described.[5]

Statistical analysis. Regarding differences between the plaque and non-plaque types, gender compositions, site of dura mater grafting, occurrence of initial symptoms and occurrence of manifestations, rate of positive findings on tests were assessed by χ^2 test, and age at dura mater grafting, incubation period from dura mater grafting until onset of CJD, age at onset, duration between the onset and occurrence of each manifestation, duration between onset and death by the Mann-Whitney test. Significance was defined as $p < 0.05$. The analyses were performed using Stat View J-7.5 (Abacus Concepts, Berkeley, CA).

Ethical issues. All patients' families gave their informed consent to participate in the study. The study protocol was approved by the Institutional Ethics Committee.

Table 1 Demographic features of pathologically confirmed dura mater graft-associated Creutzfeldt-Jakob disease (dCJD) for total patients, patients with the plaque type dCJD, and patients with the non-plaque type dCJD

Feature	Total	Plaque type	Non-plaque type	p Value*
Patients (n)	25†	11	12	—
Men/women	10/15	4/7	5/7	NS
Site of dura mater graft: supra-/infratentorial‡	11/9	5/4	6/4	NS
The year of dura mater graft (range)	1979–1988	1982–1988	1983–1987	—
Age at dura mater grafting, y, mean ± SD (range)	40.7 ± 17.0 (9–64)	39.2 ± 16.4 (9–58)	41.7 ± 19.5 (16–64)	NS
Incubation period,§ y, mean ± SD (range)	14.8 ± 2.8 (9–21)	14.6 ± 2.4 (9–17)	14.6 ± 3.4 (11–21)	NS
Age at onset, y, mean ± SD (range)	56.5 ± 15.3 (28–76)	55.8 ± 15.4 (28–59)	56.7 ± 17.1 (30–76)	NS

*p Value was assessed between the plaque and non-plaque types.
†The patients included two patients in whom sufficient pathological data were not available to be classified to the plaque or non-plaque type.
‡In some patients, precise information for the site of dura mater graft was not available.
§Incubation period: duration between the dura mater grafting and onset of CJD.

RESULTS dCJD in Japan. CJD surveillance in Japan has identified 766 patients with prion diseases during the last 7 years. sCJD was found in 592 patients (77.3%), inherited prion diseases in 104 (13.6%), environmentally acquired prion diseases in 67 (8.7%), and unclassified prion diseases in 3. The environmentally acquired prion diseases consisted of 66 patients with dCJD and one case of vCJD.[18] Combined with dCJD patients identified by the previous surveillance systems,[3] the total number of dCJD patients in Japan is 122 to date. According to the vital statistics of the Ministry of Health, Labor and Welfare, Japan, that had been published for the data of 2004 or before,[19] the mean annual mortality rate of prion disease from 1999 to 2004 was 1.05 per 1 million people. It was estimated that about 71% of the total CJD patients with death certificates could be investigated by our current surveillance system. When the proportions of sCJD (77.3%), inherited prion disease (13.6%), and dCJD (8.6%) in total prion diseases were applied, the annual mortality rate was estimated to be 0.81 per 1 million people for sCJD, 0.15 for inherited prion diseases, and 0.09 for dCJD.

The 66 dCJD patients were classified into 25 patients with pathologic confirmation, and 41 with no pathologic confirmation but characteristic neurologic manifestations. For the source of allogenic dura mater, Lyodura® (B. Brown, Germany) was used in all the dCJD patients in which the brand name of dura mater could be identified; little was known about lot numbers or size of cadaveric dura mater graft. PrP gene analysis did not detect any mutation in any of the patients. For polymorphisms in the PrP gene, all the examined patients showed methionine homozygosity at codon 129 and glutamic acid homozygosity at codon 219, except for a pathologically unconfirmed dCJD patient showing a methionine/valine polymorphism at codon 129 and a pathologically confirmed patient of the non-plaque type with a glutamic acid/lysine polymorphism at codon 219.

Analysis of pathologically confirmed dCJD patients. Among the 25 patients with pathologically confirmed dCJD, sufficient neuropathologic data were available in 23 patients, and they could be classified to 11 with the plaque type (48%) and 12 with the non-plaque type (52%). Plaque type PrP deposits found in the plaque type dCJD were often surrounded by a zone of spongiform changes, giving them a florid appearance. Western blot analysis of PrP^{res} using brain samples from all the patients demonstrated the type 1 pattern, according to the classification by Parchi et al.[11,12] in both the plaque and non-plaque types.

The demographic features are summarized in table 1. There was no significant difference in gender composition, site of dura mater graft, age at dura mater grafting, age at onset, or incubation periods between the dura mater grafting and onset of CJD between the plaque and non-plaque types. The years in which neurosurgical procedures were performed with dura mater grafts were not different between the two groups.

For the initial symptoms, 55% of the patients with the plaque type presented with gait disturbance, commonly ataxia, while patients with the non-plaque type showed a variety of initial symptoms. There was no apparent relation between the site of dura mater graft and initial symptoms (data not shown).

Table 2 Manifestations of pathologically confirmed dura mater graft-associated Creutzfeldt-Jakob disease (dCJD) for total patients, patients with the plaque type dCJD, and patients with the non-plaque type dCJD

	Total (n = 25)*		Plaque type (n = 11)		Non-plaque type (n = 12)		p Value†	
	Occurrence (%)	Duration†	Occurrence (%)	Duration†	Occurrence (%)	Duration†	Occurrence	Duration†
Cerebellar signs	80	1.8 ± 2.7	91	2.2 ± 2.7	75	0.6 ± 1.0	NS	NS
Psychiatric symptoms	60	1.0 ± 1.7	55	1.4 ± 2.6	67	0.5 ± 0.7	NS	NS
Dementia	100	2.6 ± 3.2	100	4.0 ± 3.5	100	0.9 ± 0.9	—	<0.01
Visual disturbance	52	3.5 ± 3.8	64	5.7 ± 3.5	42	0.4 ± 0.5	NS	<0.0001
Myoclonus	88	4.4 ± 3.1	73	7.3 ± 1.7	100	2.0 ± 1.3	0.052	<0.01
Extrapyramidal signs	60	5.8 ± 3.9	82	7.3 ± 3.6	42	2.2 ± 1.0	<0.05	<0.0001
Pyramidal signs	72	4.5 ± 3.1	45	8.2 ± 1.6	100	2.2 ± 1.4	<0.005	<0.0001
Akinetic mutism	84	6.1 ± 4.5	73	10.3 ± 3.2	92	2.8 ± 1.2	NS	<0.0001
Death§	100	15.8 ± 9.2	100	13.3 ± 6.6	100	17.9 ± 11.5	—	NS

*The patients included two patients in whom sufficient pathologic data were not available to be classified to the plaque or non-plaque type.
†Duration between the onset and occurrence of each manifestation. Duration (months) is expressed as mean ± SD.
‡p Value was assessed between the plaque type and non-plaque type of dCJD.
§In Japan, most of the dCJD patients at the stage of akinetic mutism were managed carefully with supportive therapies until death; the duration between onset and death is not influenced by the disease progression.

Regarding clinical manifestations (table 2), the plaque type showed lower frequencies of myoclonus and pyramidal sign, higher frequencies of extrapyramidal sign, and significantly later occurrence of dementia, visual disturbance, myoclonus, pyramidal/extrapyramidal sign, and akinetic mutism, in comparison with the non-plaque type. However, the duration between onset of CJD and death was not different between the plaque and non-plaque types, because most of the patients had received careful therapies to support general conditions even at the stage of akinetic mutism until death. The interval between onset and cerebellar signs was shorter than that of other manifestations in patients with the plaque type. Thus, the plaque type was generally characterized by onset with progressive gait disturbance, mainly ataxia, and a relatively long clinical course.

Regarding laboratory and MRI tests (table 3), only 1 (9%) of the patients with the plaque type showed late occurrence (13 months after onset) of PSWCs on EEG; in contrast, all patients with the non-plaque type showed PSWCs within 5 months. For CSF markers, positive 14-3-3 protein and elevation of NSE were frequently found in the plaque as well as non-plaque types, and the positive rates were not significantly different between the two groups. Concerning MRI studies, hyperintense lesions on T2WI, FLAIR images, or DWI, which are diagnostic for CJD, were found in 67% of the plaque type, and in 82% of the non-plaque type; when confined to the patients examined by DWI, all patients with either plaque or non-plaque type showed high intensity signals.

Analysis of clinically diagnosed dCJD patients. In analysis of 41 patients without pathologic confirmation of dCJD, 7 patients were excluded because our investigation was performed less than 12 months after the onset of CJD. Consequently, 34 patients were analyzed in this study including 27 with PSWCs(+) and 7 with PSWCs(−) dCJD.

There were no significant differences between the PSWCs(+) and PSWCs(−) groups, in gender distribution, site of dura mater graft, year of dura mater grafting, age at dura mater grafting, age at onset of CJD, the incubation period, or the duration between onset of CJD and death (data not shown). Regarding clinical features, the PSWCs(−) group showed significantly higher frequency of gait disturbance (commonly ataxia) as an initial symptom, significantly lower frequencies of myoclonus and akinetic mutism, and significantly later occurrence of dementia, psychiatric symptoms, visual disturbance, myoclonus, and akinetic mutism, in comparison with the PSWCs(+) group (data not shown). Thus, the PSWCs(−) group commonly showed onset with ataxic gait disturbance and relatively slow progression; these clinical features of the PSWCs(−) group were similar to those of the plaque type, while the clinical features of the PSWCs(+) group were similar to those of the non-plaque type char-

Table 3 Laboratory and MRI findings of pathologically confirmed dura mater graft-associated Creutzfeldt-Jakob disease (dCJD) for total patients, patients with the plaque type, and patients with the non-plaque type of dCJD

	Total patients (n = 25)*		Plaque type (n = 11)		Non-plaque type (n = 12)		
	No. of examined patients	No. (%) of patients with positive	No. of examined patients	No. (%) of patients with positive	No. of examined patients	No. (%) of patients with positive	p Value†
EEG							
PSWCs	25	15 (60)	11	1‡ (9)	12	12‡ (100)	<0.0001
CSF							
Positive 14-3-3 protein	13	11 (85)	4	3 (75)	8	7 (88)	NS
Elevated levels of NSE	12	10 (83)	4	4 (100)	7	6 (86)	NS
MRI§							
T2WI, FLAIR images, or DWI	22	16 (73)	9	6 (67)	11	9 (82)	NS
DWI	7	7 (100)	3	3 (100)	4	4 (100)	NS
PrP genotype							
Codon 129 polymorphism	20	MM 20	9	MM 9	10	MM 10	—
Codon 219 polymorphism	19	EE 18	9	EE 9	10	EE 9	—
		EK 1				EK 1	—

*The patients included two patients in whom sufficient pathologic data were not available to be classified to the plaque or non-plaque type.
†*p* Value was assessed between the plaque and the non-plaque type.
‡Duration from onset to appearance of PSWCs on EEG was 13 months in a patient with the plaque type, and 1 to 5 (mean [SD] 2.3 [1.0]) months in the non-plaque type dCJD.
§We evaluated hyperintense lesions in the basal ganglia, thalamus, and cortical ribbons on diffusion-weighted image (DWI), fluid-attenuated inversion recovery (FLAIR) images, or T2 weighted images (T2WI).
PSWCs = periodic sharp wave complexes; NSE = neuron specific enolase; MM = methionine homozygosity; EE = glutamic acid homozygosity; EK = glutamic acid/lysine heterozygosity.

acterized by classic CJD features. Although all patients of the PSWCs(+) group showed the PSWCs on EEG within 7 months, only one patient of the PSWCs(−) group showed PSWCs on EEG 15 months after onset. CSF markers (14-3-3 protein and NSE) and DWI of MRI showed high rates of positivity (75 to 100%) in both the PSWCs(+) and PSWCs(−) dCJD groups (table 4).

DISCUSSION Our study demonstrated that the plaque type was found in 48% of pathologically confirmed dCJD patients, and was characterized by onset with progressive gait disturbance (mostly ataxia), significantly later development of myoclonus and akinetic mutism, and no or late occurrence of PSWCs on EEG; the features were quite different from the classic CJD features of the non-plaque type. Importantly, investigations with MRI, especially DWI, and CSF markers (14-3-3 protein and NSE) showed high rates of positive diagnostic findings for the plaque as well as the non-plaque types. The analyses of clinical manifestations and laboratory findings in the pathologically confirmed and pathologically unconfirmed dCJD patients indicated that the features of the PSWCs(−) dCJD group were similar to those of the plaque type, and the features of the PSWCs(+) dCJD group to those of the non-plaque type; it is likely that the pathologic background of the PSWCs(−) dCJD group would be mostly PrP plaque-forming pathology, i.e., the plaque type, and that of the PSWCs(+) dCJD group would be mostly synaptic type PrP deposits without plaque formation, i.e., the non-plaque type.

Including the 66 patients with dCJD identified under the current surveillance system, the total number of dCJD patients in Japan was calculated to be 122 in February 2006. The analysis of 23 patients with pathologically confirmed dCJD demonstrated that the frequency of the plaque type in dCJD was 48%. However, as the plaque type was associated with atypical clinical features, it is possible that patients with the plaque type might be more frequently autopsied than the non-plaque type with classic CJD features, i.e., a selection bias for autopsy. In the analysis of 34 patients with pathologically unconfirmed dCJD, the PSWCs(−) dCJD with atypical clinical features, probably corresponding to the plaque type, was found in 7 patients (21%). On the assumption that the PSWCs(−) dCJD would represent

Table 4 Laboratory and MRI findings of clinically diagnosed dura mater graft-associated Creutzfeldt-Jakob disease (dCJD) for total patients, patients with the PSWCs(+) category, and patients with the PSWCs(−) category

	Total patients (n = 41)*		PSWCs(+) dCJD (n = 27)		PSWCs(−) dCJD (n = 7)		
	No. of examined patients	No. (%) of patients with positive	No. of examined patients	No. (%) of patients with positive	No. of examined patients	No. (%) of patients with positive	p Value†
EEG							
PSWCs	41	28 (68)	27	27‡ (100)	7	1‡ (14)	<0.0001
CSF							
Positive 14-3-3 protein	10	10 (100)	7	7 (100)	1	1 (100)	NS
Elevated levels of NSE	17	16 (89)	12	12 (100)	4	3 (75)	NS
MRI§							
T2WI, FLAIR images, or DWI	26	18 (69)	18	13 (71)	4	2 (50)	NS
DWI	8	7 (88)	5	5 (100)	0	0	—
PrP genotype							
Codon 129 polymorphism	26	MM 25 MV 1	18	MM 17 MV 1	8	MM 8	—
Codon 219 polymorphism	25	EE 25	17	EE 17	8	EE 8	—

*The 41 patients included 27 with PSWCs(+) dCJD and 14 with PSWCs(−) dCJD; 7 with PSWCs(−) dCJD were excluded from the analysis because they were investigated within 12 months after the onset.
†*p* Value was assessed between the PSWCs(+) and PSWCs(−) categories.
‡Duration from onset to appearance of PSWCs on EEG was 1 to 7 (mean ± SD, 2.6 ± 1.4) months in the PSWCs(+), and 15 months in a patient with the PSCWs(−) dCJD.
§We evaluated high intensity lesions in the basal ganglia, thalamus, and cortical ribbons on diffusion-weighted image (DWI), fluid-attenuated inversion recovery (FLAIR) images, or T2 weighted images (T2WI).
PSWCs(+) dCJD = dCJD which showed periodic sharp wave complexes within 12 months after onset; PSWCs(−) dCJD = dCJD which did not show PSWCs within 12 months after onset; NSE = neuron specific enolase; MM = methionine homozygosity; EE = glutamic acid homozygosity; EK = glutamic acid/lysine heterozygosity.

the plaque type and PSWCs(+) dCJD non-plaque type, we can combine the PSWCs(−) dCJD patients (n = 7) with the plaque type (n = 11). As a result, the total number of plaque type dCJD patients is 18, and the proportion of the plaque type dCJD patients in all the plaque and non-plaque type dCJD patients (n = 57) is calculated to be 32%. Thus, one-third of dCJD patients may be the plaque type.

In a previous report about dCJD patients in Japan based on data from the previous investigation systems, 3 (25%) of 12 patients with pathologically confirmed dCJD showed plaque formation in the brain, although the frequency of clinically atypical patients was not described.[3] Another study of dCJD in Japan reported that 15% of dCJD patients presented with atypical clinical features.[4] Thus, our current study demonstrated that the frequency of the plaque type (clinicopathologically, atypical form) among all dCJD patients would be higher than previously recognized.

There are possible explanations for the higher frequency of plaque type dCJD. First, according to publications focusing on the plaque type or atypical form of dCJD,[3-9] recognition of this peculiar type might be increased. Second, the incubation periods after dura mater grafting to CJD onset differ between the previous study and the current study, and this might be related to the increased proportion of the plaque type; in the previous study,[3] the incubation period was 8.2 ± 3.8 (mean ± SD) years for dCJD patients, while our current study showed a longer incubation period (14.8 ± 2.8 years) for pathologically confirmed dCJD patients. If the plaque type is associated with a longer incubation period compared with the non-plaque type, the current surveillance data of dCJD patients with a longer incubation period would present with more patients with the plaque type. However, this hypothesis, i.e., "the longer incubation period in the plaque type," is not supported by our results, because there was no difference in the incubation period between the plaque and non-plaque types.

Further, our results could not demonstrate a difference between the plaque and non-plaque types with regard to factors related to the dura mater grafting or recipients. Regarding dura mater graft–related factors, Lyodura® was used in all the dCJD patients in whom the brand name of

dura mater graft could be identified, irrespective of the plaque or non-plaque types; there was no information on the donors of the dura mater product available at all. No clustering of the plaque type patients was observed for the years in which neurosurgical procedures with dura mater grafting were performed. However, a recent transmission study with brain samples from the plaque type dCJD to knock-in-mice that had human PrP with methionine at codon 129 suggested the presence of a specific prion strain that could cause type I PrP^{res} accumulation with plaque formation.[20] Regarding recipient-related factors, the gender distribution, age at dura mater grafting, or sites of dura mater grafting did not differ between the plaque and non-plaque types. In both the plaque and non-plaque types (table 3), polymorphic codons 129 and 219 were methionine homozygosity and glutamic acid homozygosity, except for a non-plaque type dCJD patient with a glutamic acid/lysine polymorphism at codon 219. Regarding pathologically unconfirmed dCJD patients, a patient with the PSWCs(+) dCJD, probably the non-plaque type, had a methionine/valine polymorphism at codon 129 (table 4). In addition, both the plaque and non-plaque types presented with type 1 PrP^{res}. Further investigations with a larger number of pathologically verified patients are necessary to better understand the factors that contribute to the development of plaque or non-plaque type of dCJD.

Importantly, our findings indicated that MRI, especially DWI, and CSF markers (14-3-3 protein and NSE) would provide high diagnostic sensitivities in the plaque as well as the non-plaque type for pathologically confirmed patients (table 3), and in both the PSWCs(+) and PSWCs(−) categories for clinically diagnosed dCJD patients (table 4), although the studies with CSF 14-3-3 protein or DWI of MRI were limited to a small number of dCJD patients. It has been reported that the diagnostic sensitivity of CSF 14-3-3 protein is relatively low in CJD patients with long disease duration compared to that in those showing a typical clinical course.[21] Since in our current study, CSF 14-3-3 protein was investigated only in four patients with plaque type dCJD, showing positive results in 3 patients (75%), further study with a larger number of the plaque type dCJD patients would be required to confirm the diagnostic value of CSF 14-3-3 protein.

To facilitate clinical diagnosis of plaque type dCJD for patients in which CSF 14-3-3 protein test is negative at the time of diagnosis or not available, we propose that "progressive ataxia in human cadaveric dura mater recipients" can be categorized as probable dCJD. This is similar to the diagnostic criteria for probable iCJD associated with human pituitary hormones defined by progressive cerebellar syndrome (WHO 2003).[22] The revision of the iCJD diagnostic criteria[22] for dCJD would allow appropriate classification of the great majority but not all patients of the plaque type.

ACKNOWLEDGMENT

The authors thank Drs. Fumio Moriwaka, Yoshiyuki Kuroiwa, Masatoyo Nishizawa, Nobuo Sanjyo, Masatoshi Takeda, Yusei Shiga, Shigetoshi Kuroda, Shigeki Kuzuhara, Jun Tateishi, Hiroyuki Murai, and Shigeo Murayama for the CJD surveillance. The CJD Surveillance Committee belongs to the Research Group of Prion Disease and Slow Virus Infection, funded by the Ministry of Health, Labor and Welfare, Japan. The funding source had no involvement in the process of this publication.

Received October 20, 2006. Accepted in final form February 27, 2007.

REFERENCES

1. Brown P, Brandel JP, Preece M, Sato T. Iatrogenic Creutzfeldt–Jakob disease. The waning of an era. Neurology 2006;67:389–393.
2. Thadani V, Pernar PL, Partington J, et al. Creutzfeldt–Jakob disease probably acquired from a cadaveric dural mater graft. J Neurosurg 1988;69:766–769.
3. Hoshi K, Yoshino H, Urata J, Nakamura Y, Yanagawa H, Sato T. Creutzfeldt–Jakob disease associated with cadaveric dural mater grafts in Japan. Neurology 2000;55: 718–721.
4. Sato T, Masuda M, Utsumi Y, et al. Dural mater related Creutzfeldt–Jakob disease in Japan: relationship between sites of grafts and clinical features. In: Prions: food and drug safety. Tokyo: Springer, 2005;31–40.
5. Shimizu S, Hoshi K, Muramoto T, et al. Creutzfeldt–Jakob disease with florid-type plaques after cadaveric dural mater grafting. Arch Neurol 1999;56:357–362.
6. Kopp N, Streichenberger N, Deslys JP, Laplanche JL, Chazot G. Creutzfeldt–Jakob disease in a 52-year-old woman with florid plaques. Lancet 1996;348:1239.
7. Takashima S, Tateishi J, Taguchi Y, Inoue H. Creutzfeldt–Jakob disease with florid plaques after cadaveric dura graft in a Japanese woman. Lancet 1997; 350:865–866.
8. Kimura K, Nonaka A, Tashiro H, et al. Atypical form of dura graft-associated Creutzfeldt–Jakob disease: report of a postmortem case with review of the literature. J Neurol Neurosurg Psychiatry 2001;70:696–699.
9. Satoh K, Muramoto T, Tanaka T, et al. Association of an 11-12kDa protease-resistant prion protein fragment with subtypes of dural graft-associated Creutzfeldt–Jakob disease and other prion diseases. J Gen Virol 2003;84:2885–2893.
10. Will RG, Ward HJ. Clinical features of variant Creutzfeldt–Jakob disease. Curr Top Microvirol Immunol 2004;284:121–132.
11. Parchi P, Castellani R, Capellari S, et al. Molecular basis of phenotypic variability in sporadic Creutzfeldt–Jakob disease. Ann Neurol 1996;39:767–778.

12. Parchi P, Capellari S, Chen SG, et al. Typing prion isoforms. Nature 1997;386:232–234.
13. Nishida N, Yamada M, Hara K, et al. Creutzfeldt–Jakob disease after Jannetta's operation with cadaveric dura mater graft: initial manifestations related to the graft site. J Neurol 2002;249:480–483.
14. Shiga Y, Miyazawa K, Sato S, et al. Diffusion-weighted MRI abnormalities as an early diagnostic marker for Creutzfeldt–Jakob disease. Neurology 2004;63: 443–449.
15. Aksamit AJ, Preissner CM, Homburger HA. Quantitation of 14-3-3 and neuron-specific enolase proteins in CSF in Creutzfeldt–Jakob disease. Neurology 2001;57: 728–730.
16. Kitamoto T, Shin RW, Doh-ura K, et al. Abnormal isoform of prion protein accumulates in the synaptic structures of the central nervous system in patients with Creutzfeldt–Jakob disease. Am J Pathol 1992;140: 1285–1294.
17. Kitamoto T, Ohta M, Doh-ura K, Hitoshi S, Terao Y, Tateishi J. Novel missense variants of prion protein in Creutzfeldt–Jakob disease or Gerstmann-Sträusller syndrome. Biochem Biophys Res Commun 1993;191: 709–714.
18. Yamada M, on behalf of the Variant CJD Working Group, Creutzfeldt–Jakob Disease Surveillance Committee, Japan. The first Japanese case of variant Creutzfeldt–Jakob disease showing periodic electroencephalogram. Lancet 2006;367:874.
19. Statistics and Information Department, Ministers Secretariat, Ministry of Health, Labour and Welfare: Vital statistics of Japan 1999–2004. Tokyo: Health and Welfare Statistics Association, 2006.
20. Mohri S, Kitamoto T, Miyoshi I, Matsuura Y. Estimation for a novel knock-in mouse as rapid and sensitive bioassay system for human prions [in Japanese with English abstract]. Annual Report of the Prion Disease and Slow Virus Infection Research Committee. 2004: 141–145.
21. Van Everbroeck B, Quoilin S, Boons J, Martin JJ, Cras P. A prospective study of CSF markers in 250 patients with possible Creutzfeldt–Jakob disease. J Neurol Neurosurg Psychiatry 2003;212:1210–1214.
22. WHO manual for surveillance of human transmissible spongiform encephalopathies including variant Creutzfeldt–Jakob disease. Published 2003. Available at: www.who.int/bloodproducts/tse/en/. Accessed January 6, 2007.

Acta Neuropathol (2007) 113:627–636
DOI 10.1007/s00401-007-0211-z

ORIGINAL PAPER

Amyloid precursor protein cytoplasmic domain with phospho-Thr668 accumulates in Alzheimer's disease and its transgenic models: a role to mediate interaction of Aβ and tau

Ryong-Woon Shin · Koichi Ogino · Alfredo Shimabuku · Takao Taki · Hanae Nakashima · Takeshi Ishihara · Tetsuyuki Kitamoto

Received: 15 November 2006 / Revised: 18 February 2007 / Accepted: 19 February 2007 / Published online: 13 March 2007

Abstract Abnormal accumulation of Aβ and tau in senile plaques (SP) and neurofibrillary tangles (NFTs) is a key event in Alzheimer's disease (AD). Here, we show that T668-phosphorylated cytoplasmic domain of APP (pT668-ACD) accumulates Aβ and tau in AD and its transgenic models. Anti-pT668 immunostaining of AD brain sections with hydrated autoclave enhancement identified SP neurites and NFTs in which pT668-ACD colocalizes with tau. We produced and examined transgenic (Tg) mice that overexpress human APP695, harboring the double Swedish/London mutation, and develop age-dependently Aβ plaques in the brain. All Aβ plaques contain co-accumulations of pT668-ACD, but co-accumulation of tau appears in only a fraction of Aβ plaques in older animals. We also examined the established tau Tg mice that overexpress the smallest human brain tau isoform and develop neuronal accumulations of tau in older animals. Examination of the old tau Tg mice showed that neuronal cells affected by tau accumulation induce co-accumulation of pT668-ACD. We speculate that in AD brains, extracellular Aβ deposition is accompanied by intracellular accumulation of pT668-ACD, followed by tau accumulation in the SP with dystrophic neurites and that neuronal cells affected by tau accumulation induce co-accumulation of pT668-ACD in NFTs. Thus, pT668-ACD is likely to mediate pathological interaction between Aβ and tau.

Keywords Tau · Aβ · Alzheimer's disease · APP · Transgenic mice

R.-W. Shin (✉)
Department of Neurological Science,
Tohoku University Graduate School of Medicine,
2-1 Seiryo-machi, Sendai 980-8575, Japan
e-mail: shin@mail.tains.tohoku.ac.jp

K. Ogino · A. Shimabuku · T. Taki
Molecular Medical Science Institute,
Otsuka Pharmaceutical Co., Ltd, Tokushima, Japan

H. Nakashima · T. Ishihara
Department of Neuropsychiatry,
Okayama University Graduate School of Medicine,
Okayama, Japan

T. Kitamoto
Division of CJD Science and Technology,
Department of Prion Research,
Center for Translational and Advanced Animal Research
on Human diseases, Tohoku University Graduate
School of Medicine, Sendai 980-8575, Japan

Introduction

Senile plaques (SPs) and neurofibrillary tangles (NFTs) are two hallmark pathological features that characterize the brains affected by Alzheimer's disease (AD). Both lesions result from the pathological deposition of proteins that normally distribute throughout the brain. SPs are extracellular deposits of fibrillar amyloid β peptide (Aβ), a cleavage product of the amyloid precursor protein (APP) [26]. NFTs are intracellular aggregated bundles of hyperphosphorylated tau protein. These two lesions are often present in the same brain areas, suggesting that there might be a mechanistic link between them. Further, extracellular Aβ deposits, especially those in the mature form of cored plaques, are accompanied by surrounding dystrophic neurites in which hyperphosphorylated tau accumulates [5, 27]. Notably, recent studies have shown that APP/Aβ influences the formation of NFT-like tau aggregates in transgenic mice expressing an FTDP-17-causing tau mutant [9, 20], suggesting that they may be functionally linked. Thus, it is

likely that SPs and NFTs are not independent neuropathologic entities, but instead that these lesions and their constituent molecules APP/Aβ and tau are pathogenically related to each other.

Aβ is produced within the lumen of the cell following cleavages of membrane-associated APP and secreted extracellularly, while tau is a microtubule-associated cytoskeletal protein located in the cytosol. Therefore, under physiological conditions, these two molecules probably do not encounter each other in the same cellular compartments. On the contrary, the cytoplasmic domain of APP could interact directly or indirectly with tau.

Threonine 668 (T668) in the cytoplasmic domain of APP is a known in vivo phosphorylation site [24]. The phosphorylation at T668 of APP regulates the APP processing in such a way as to increase Aβ production [1, 3, 19], and therefore Aβ production and T668 phosphorylation of APP are linked. On the other hand, Aβ was shown to mediate phosphorylation of tau [2, 6, 33], indicating a possibility that phosphorylation of tau and T668 phosphorylation of APP are linked. Furthermore, tau and T668 of APP are the targets of the same protein kinases, including CDK5, GSK3β and SAPK/JNK [4, 8, 12, 13, 32]. We therefore hypothesize that APP cytosolic domain with phospho-Thr668 (pT668-ACD) interacts with tau and this interaction might mediate the functional link between Aβ and tau. To test our hypothesis, we performed immunohistochemical analysis of AD brains and showed that pT668-ACD accumulates in SP neurites and NFTs in association with tau. To understand if there is a relationship between the accumulations of pT668-ACD and tau, we examined transgenic models for SPs and for NFTs. We obtained evidence that extracellular deposition of Aβ is accompanied by intracellular accumulation of pT668-ACD in dystrophic neurites surrounding SPs, followed by accumulation of tau, and that neuronal cells affected by tau accumulation induce co-accumulation of pT668-ACD. These results indicate that there are reciprocal relationships between accumulations of pT668-ACD and tau. We propose a role for pT668-ACD in mediating interaction between Aβ and tau.

Materials and methods

Generation of transgenic mice

The prion protein (PrP) transgenic (Tg) vector composed of the combined 129/Sv and I/Ln mouse prion protein genes [17] was modified to serve as a universal tool to produce Tg mice expressing other target proteins (Fig. 1a). The entire open reading frame located in exon 3 that encodes mouse PrP was deleted and replaced by a ClaI endonuclease site that was created. A cDNA of human *APP695* with epitopic tag BE7 introduced immediately after the signal peptide [31] was subjected to site-directed mutagenesis to harbor either the Swedish (*BE-APP695*$_{Sw}$), London (*BE-APP695*$_{Lo}$) or double Swedish/London mutation (*BE-APP695*$_{Sw/Lo}$). After creation of the ClaI site both at the 5′ and 3′ end sites, the cDNA *BE-APP695*$_{Sw}$, *BE-APP695*$_{Lo}$ or *BE-APP695*$_{Sw/Lo}$ was introduced into the ClaI-digested Tg vector. Tg mice were generated on a C57BL/6 background. Of five founders obtained as assessed by PCR and Southern blotting of tail DNA, line 1-1 for *BE-APP695*$_{Lo}$ (APP-Lo 1-1) as well as lines 7-5 and 7-9 for *BE-APP695*$_{Sw/Lo}$ (APP-SL 7-5 and APP-SL 7-9) were found to overexpress human APP695 (see Results), and these three lines were expanded and used for further experimentation. Mice from these three lines displayed memory disturbance as revealed by the Morris Water Maze test performed at ages ranging from 3 to 12 months. Notably, mice from APP-Lo 1-1 exhibited invariable memory disturbance with less deviations among the animals examined. As mice from APP-Lo 1-1 begin to develop Aβ deposition in older animals (at ages 15 months and over) and with less severity than those from APP-SL 7-5 and 7-9, they were excluded from the current immunohistochemical study. Tg mice overexpressing human APP with the Swedish mutation, Tg2576 (HuAPP695, K670N/M671L) [11], were purchased from Taconic (NY) and used in this study for comparison. The tau transgenic mice overexpressing the smallest human brain tau isoform [14] were also used.

Tissue preparation

The transgenic mice as well as non-transgenic C57BL/6 mice were euthanized with ether and perfused transcardially with saline. The brains were rapidly removed and bisected through the mid-sagittal plane into each hemisphere. The lateral hemispheres were immersed in 10% buffered formalin for 2–3 days and embedded in paraffin for immunohistochemical analysis. The other hemispheres were frozen for subsequent use in immunoblot analysis and sandwich enzyme-linked immunosorbent assays (ELISA).

Immunoblot and ELISA

For immunoblotting, the frozen mouse brain hemisphere was homogenized in 9 volumes of 0.1 M Tris pH 7.6/0.1M NaCl, including protease inhibitor cocktails (Roche Applied Science, Indianapolis, IN, USA), and centrifuged at 600×*g* for 5 min. The supernatant was centrifuged at 100,000×*g* for 1 h at 4°C, and the membrane fraction recovered in the pellet was resolved in 10 mM Tris pH 7.6/2% SDS. The protein concentration was quantified by BCA assay (Pierce, Rockford, IL, USA), and immunoblotting was performed with monoclonal antibody (Mab) BE11 [25] that recognizes the BE7 epitope tagged at the N-terminus of

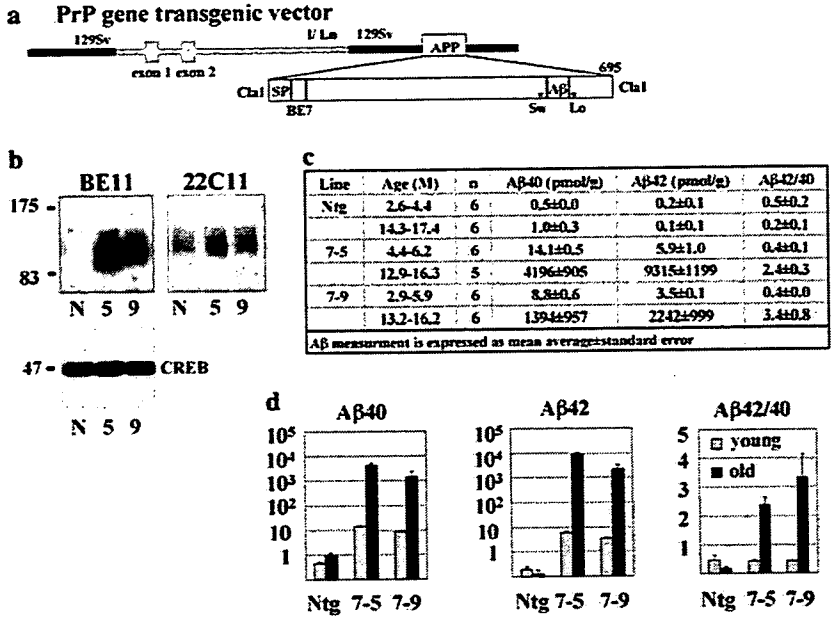

Fig. 1 Generation and primary characterization of APP-SL Tg mice. **a** Structure of BE7-tagged human APP695 with both the Swedish-(*Sw*) and London-type (*Lo*) familial AD mutations (denoted by *) linked to the mouse PrP gene transgenic vector consisting of combined 129/Sv (*in black*) and I/Ln (*in gray*) genes. **b** Western blot analysis of the brains from APPSL Tg 7-5 (5) and 7-9 (9) lines in comparison with that from the non-transgenic littermate (N) using BE11 (*upper left panel*) and 22C11(*upper right panel*). The brain sample containing 50 μg of total protein is loaded in each lane. CREB was detected by anti-CREB antibody (Upstate, NY) as the internal control (*lower panel*). The position of Mr markers is indicated in kilodaltons. **c**, **d** Results of ELISA for Aβ40 and Aβ42 produced in the brains from non-transgenic littermates (*Ntg*) and APPSL Tg 7-5 and 7-9 lines and calculated ratio of Aβ42 to Aβ40 (Aβ42/40). The results were obtained based on animals divided into young and old groups. Here Aβ was measured by the ELISA kit specific for human Aβ. When the ELISA kit for human and mouse Aβ (IBL, Japan) is used, the values of Aβ are slightly higher in non-transgenic mice, while, in transgenic mice, the values of Aβ are not prominently different from those measured by the human Aβ ELISA kit (supplementary material)

APP immediately after its signal peptide [31] and monoclonal antibody (Mab) 22C11 specific to the N-terminal portion of APP [35]. For Aβ ELISA, the mouse brain homogenate was centrifuged at 350,000×*g* for 20 min at 4°C. The supernatant was used as the soluble fraction. The pellet was solubilized by sonication in 4 volumes of 6 M guanidine–HCl in 50 mM Tris–HCl pH 7.6 and centrifuged once again at 200,000×*g* for 20 min at 4°C. The guanidine–HCl supernatants were diluted over 20 times to reduce the concentration of guanidine–HCl and used as the insoluble fraction. Levels of transgenic human Aβ40 and Aβ42 in the soluble and insoluble fractions were quantified by ELISA using the human Aβ ELISA kit (IBL, Japan).

Immunohistochemistry

Coronal sections were cut at 5-μm thickness from brains of neuropathologically confirmed AD patients ($n = 8$, age 63–79 years) and nondemented patients ($n = 5$, age 64–88 years), showing no significant pathology on routine neuropathologic examination, as well as those of Tg and non-Tg animals. The Tg animals examined included APP-SL Tg 7-5 line aged 3 ($n = 3$), 6 ($n = 6$), 9 ($n = 3$), 12 ($n = 2$), 15 ($n = 3$) and 18 ($n = 1$) months and 7-9 line aged 3 ($n = 3$), 6 ($n = 3$), 9 ($n = 3$), 12 ($n = 3$), 15 ($n = 3$), 18 ($n = 4$) and 22 ($n = 1$) months, as well as non-Tg C57BL/6 mice aged 3 ($n = 3$), 5 ($n = 3$), 8 ($n = 3$), 12 ($n = 3$), 14 ($n = 4$) and 17 ($n = 4$) months. Tg2576 aged 12 ($n = 3$) and 15 months ($n = 4$), as well as the old tau Tg mice aged 32 months ($n = 3$), were also included. A series of adjacent sections were immunostained as described [23] using antibodies to Aβ including rabbit polyclonal antibody (Pab) 4702 and mouse Mab 4G8 (Senetek, Maryland Heights, MO, USA), phosphorylation-independent Mab to tau TAU-5 (BD Biosciences), phosphorylation-dependent antibodies to tau including Mabs PHF1 [10, 18] and AT8 (Innogenetics, Belgium), antibodies to phosphorylated T668 of APP anti-pT668 (Cell Signaling), antibodies specific to the C-terminal portion of APP including O443 (Calbiochem) and UT18 [34] and Mab anti-ubiquitin (Chemicon, Temecula, CA, USA). 4702 was generated in rabbits by injecting synthetic peptide corresponding to human Aβ1–40 and proved reactive both to Aβ1–40 and Aβ1–42 on ELISA (not shown). Anti-pT668 is a key antibody used in this study and re-evaluated for its specificity to phosphorylated T668 of the APP cytoplasmic domain (Fig. 2). To use for the characterization, were expressed in HEK293 cells wild-type C99 and C99 mutants in which the known in vivo

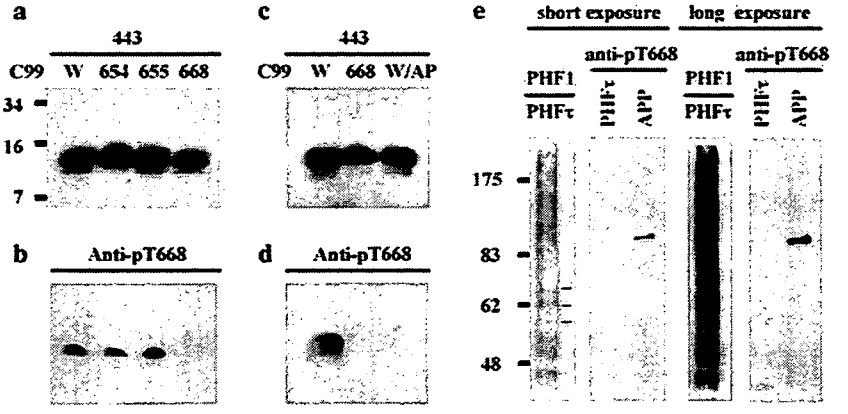

Fig. 2 Characterization of anti-pT668. **a–d** Western blot analysis of cell lysates of HEK293 cells transfected with *wild type C99* (W) and *C99 mutants* in which the known in vivo phosphorylation sites Thr654, Ser655 and Thr668 were changed to Val (654), Ala (655) and Val (668), respectively, using O443 (**a**, **c**) and anti-pT668 (**b**, **d**). The aliquots of *wild type C99*-transfected cell lysates were dephosphorylated with alkaline phosphatase prior to loading on the gel (W/AP). **e** The anti-pT668 was checked for lack of cross-reaction to PHFτ extracted from AD brain by Western blotting

phosphorylation sites T654, S655 and T668 were changed to Val (T654V), Ala (S655A) and Val (T668V), respectively [1]. Detergent-soluble cell lysates containing transfection-related wild-type C99 and C99 mutants were collected following centrifugation at 100,000×*g* for 30 min at 4°C of the homogenized cells with lysis buffer (10 mM Tris pH 7.6, 100 mM NaCl, 0.5% Triton X-100, 0.5% deoxycholic acid, 1 mM EDTA) containing protease inhibitor cocktail (Roche). Some aliquots of the sample containing wild-type C99 were treated with 1 M Tris pH 8.0 and 5 mM $ZnSO_4$, containing 24 units/ml of *E. coli* alkaline phosphatase type III (Sigma, St. Louis, MO, USA) as described [30]. The antibody was examined for its reaction to wild type C99 and C99 mutants by 16.5% Tris–Tricine SDS-PAGE followed by immunoblot analysis (Fig. 2). The anti-pT668 detects wild type C99 as well as T654V and S655A, while it fails to detect T668V, suggesting that anti-pT668 is dependent on T668 and independent of T654 and S655. Dephosphorylation of wild type C99 with alkaline phosphatase abolished the immunoreactivity of anti-pT668, indicating that the recognition of wild type C99 by anti-pT668 is dependent on the phosphorylation at T668. The anti-pT668 does not cross-react with hyperphosphorylated tau extracted from AD brain (Fig. 2). Thus, anti-pT668 specifically recognizes T668 of APP when it is phosphorylated. Antigen retrieval procedures include formic acid treatment [16] for 4702 and 4 G8 and hydrated autoclaving with 10 mM EDTA pH 6.0 [23, 28, 29] for all the other antibodies used. Notably, this heating procedure gave dramatic immunoreactive enhancement for anti-pT668, as was seen for the other antibodies. Selected sections were dephosphorylated with alkaline phosphatase (Sigma), as described [23], prior to immunostaining with anti-pT668. Selected sections were also double-labeled by immunofluorescence using either Mabs 4 G8, PHF1 or anti- ubiquitin combined with Pab anti-pT668, followed by staining with Alexa Fluor 568 anti-mouse IgG or Alexa Fluor 488 goat anti-rabbit IgG (Molecular Probes), as described [31]. Fluorescent images were analyzed using a Zeiss Axioplan2 microscope (Germany).

Results

High-level Aβ production in APP-SL Tg mice

Mice from APP-SL 7-5 and 7-9 lines were examined for expression level of the transgene in the brain. Immunoblot analysis using BE11 that recognizes only the transgenic APP, and 22C11 that recognizes both the transgenic and endogenous mouse APP, revealed that two founders APP-SL 7-5 and 7-9 lines are the high expressors of the transgenic APP (Fig. 1b). The brains of mice from each line were analyzed by ELISA specific for human Aβ40 and Aβ42 (Fig. 1c, d). The results were summarized based on animals divided into young (younger than 6 months of age) and old (older than 12 months of age) groups. In non-Tg mice, concentrations of Aβ40 and Aβ42 were low and there was no significant difference in the level between the young and the old groups. In APP-SL 7-5 and 7-9 Tg mice, exceedingly large amounts of Aβ40 and Aβ42 were produced from overexpressed human APP695 harboring the double Swedish/Lsondon mutation. Levels of Aβ40 and Aβ42 were 28- and 30-fold more increased in the young 7-5 Tg group and 18-fold more increased in the young 7-9 Tg group, respectively, compared to those in the young non-Tg group. In the old 7-5 Tg group, levels of Aβ40 and Aβ42 were increased ~4,000- and ~90,000-fold more compared to those in the

old non-Tg group, respectively. These increased levels of Aβ40 and Aβ42 correspond to ~300- and ~1,600-fold more rises compared to the levels in the young 7-5 Tg group. In the old 7-9 Tg group, levels of Aβ40 and Aβ42 were increased ~1,400- and ~22,000-fold more compared to those in the old non-Tg group, respectively, corresponding to ~160- and ~640-fold more rises compared to levels in the young 7-9 Tg group. Thus, prominently increased productions of Aβ40 and Aβ42 were observed in APP-SL 7-5 and 7-9 Tg mice, the level in APP-SL 7-5 being higher than that in APP-SL 7-9. As Aβ42 is a more amyloidogenic species than Aβ40, a high relative proportion of Aβ42 to Aβ40 (Aβ42/40) is a pathogenic marker to indicate susceptibility to Aβ deposition in the brain. Relative proportions of Aβ42/40 were calculated and analyzed. There was no difference in the Aβ42/40 ratios between the young and old non-Tg groups. The old 7-5 and 7-9 Tg groups displayed 12-fold and 17-fold more increased Aβ42/40 ratios, respectively, compared to the old non-Tg group, corresponding to levels increased 6-fold more than the young 7-5 Tg group and 9-fold more than the young 7-9 Tg group, respectively. Thus, APP-SL Tg mice showed increased ratio of Aβ42 to Aβ40 with aging. Our Tg construct worked to produce Aβ in such a way as to increase its total amount (Aβ40 plus Aβ42) as well as the ratio Aβ42/40, reflecting both the effects of Swedish- and London-type mutations of APP.

T668-phosphorylated APP cytoplasmic domain accumulates in AD brain

Tissue sections prepared from AD brains were immunohistochemically analyzed for the presence and distribution of T668-phosphorylated APP cytoplasmic domain (pT668-ACD) that accumulates in association with the SPs and neurofibrillary lesions consisting of NFTs, SP neurites and neuropil threads. Antibodies 4702 and 4G8 were used to identify extracellular Aβ deposits that constitute SPs (Fig. 3a), while AT8 and PHF1 were used to identify intra-

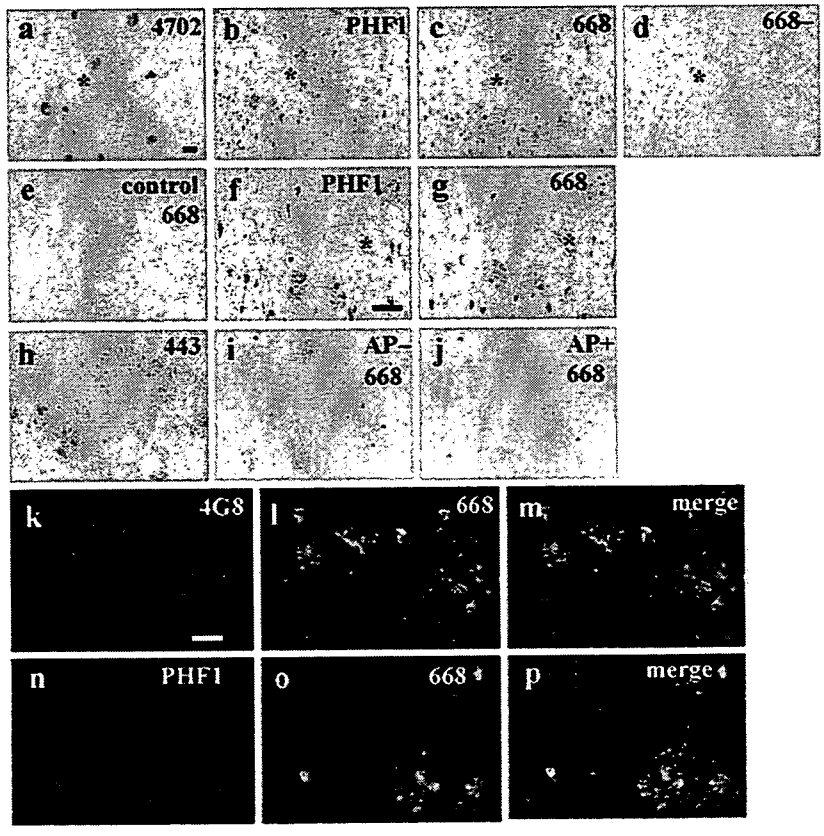

Fig. 3 Accumulation of T668-phosphorylated APP cytoplasmic domain (pT668-ACD) in dystrophic neurites of senile plaques and in neurofibrillary tangles of AD brain. All pictures are from the subiculum brain area. **a–d**, **f–j** Immunohistochemistry of serial brain sections from a 63-year-old female patient with AD using antibody to Aβ (4702) (**a**), PHF1 (**b**, **f**), anti-pT668 (668) (**c**, **g**, **i**, **j**) and O443 (443) (**h**), or without primary antibody (**d**). **f** and **g** are higher magnification pictures of **b** and **c**, respectively. *Asterisk* (*) denotes a landmark vessel to indicate the serial sections. The serial sections (**i**, **j**) were pretreated in parallel without (**i**) and with (**j**) alkaline phosphatase (*AP*). **e** Immunohistochemistry of brain section from an 88-year-old female non-demented patient (control) using anti-pT668. **k–p** Double immunofluorescence of the same AD brain sections using 4G8 (**k**) and anti-pT668 (**l**) with merged image (**m**) or using PHF1 (**n**) and anti-pT668 (**o**) with merged image (**p**). **a–e**, **f–j** and **k–p** are at the same magnifications, respectively. *Scale bars* 100 μM (**a**, **f**), 50 μM (**k**)

cellular aggregates of hyperphosphorylated tau that constitutes NFTs, SP neurites and neuropil threads (Fig. 3b, f). Massive distribution of these lesions in the hippocampus and neocortex met the established pathological hallmark of the AD brains. Immunostaining of the serial brain sections using anti-pT668 revealed immunoreactive structures that appeared to distribute in NFTs, SP neurites and neuropil threads with the same distribution pattern as displayed by AT8 and PHF1 (Fig. 3c, g). All NFTs as well as SP neurites identified by AT8 and PHF1 were positively stained by anti-pT668. The density of neuropil threads revealed by anti-pT668 appeared much less than those by AT8 and PHF1. As the diffuse form of SPs, devoid of dystrophic neuritis, was not stained by AT8 and PHF1, so were the diffuse plaques not stained by anti-pT668. For example, diffuse plaques detectable in the molecular layer of the cerebellum were not stained by anti-pT668 (not shown). Omission of anti-pT668 gave no immunoreaction, indicating its specificity (Fig. 3d). When O443 and UT-18, both of which are specific to the C-terminus of APP, were used, a minor proportion of SPs restricted to the hippocampus were labeled with the similar immunostaining profiles displayed by AT8, PHF1 and anti-pT668, suggesting that pT668-ACD in these SP neurites are intact at the C-terminus (Fig. 3h). The remaining hippocampal SPs and all SPs in the neocortex were not stained with O443 and UT-18, suggesting that pT668-ACD in these SP neurites is truncated at the C-terminus. No NFTs in the hippocampus and neocortex were stained by O443 and UT-18, indicating that pT668-ACD in NFTs are truncated at the C-terminus. Thus, NFTs and SP neurites contain pT668-ACD with the C-terminus truncated, except for a minor proportion of the SP neurites in the hippocampus that contain pT668-ACD with its intact C-terminus. To confirm that the accumulated cytoplasmic domain of APP is phosphorylated at T668, we treated AD brain sections with alkaline phosphatase prior to immunostaining with anti-pT668. Following dephosphorylation with alkaline phosphatase, the labeling of SP neurites appeared remarkably reduced, while that of NFTs appeared weakly reduced (Fig. 3i, j). When the pan-APP antibody O443 was used instead of anti-pT668 in the same experiments, no remarkable immunoreactive alterations were given before and after dephosphorylation (not shown). These results indicate that the cytoplasmic domain of APP accumulated in the SP neurites and NFTs is partly, even though not totally, phosphorylated at T668. In non-demented control brains, there were no pathological lesions detectable by the anti-Aβ and anti-tau antibodies as well as anti-pT668 (Fig. 3e). To define co-localization of pT668-ACD with Aβ and tau, double immunofluorescence was performed on the AD brain sections. Double staining by 4G8 and anti-pT668 showed that both antibodies label immunoreactive structures in SPs that appear mingled with each other, but do not merge at all, suggesting that pT668-ACD is not colocalized with extracellular Aβ deposits (Fig. 3k–m). Double immunofluorescence staining by PHF1 and anti-pT668 showed that pT668-ACD and hyperphosphorylated tau partly merge in NFTs and in the SP neurites (Fig. 3n–p). Thus, pT668-ACD co-localizes with hyperphosphorylated tau in the intracellular SP neurites and NFTs.

Age-dependent development of Aβ deposits in APP-SL Tg mice

The brains from APP-SL Tg mice of 7-5 and 7-9 lines were immunohistochemically analyzed. First, immunostaining using 4702 or 4G8 was used to evaluate the appearance and distribution of Aβ plaques. At age 3 and 6 months, there was no evidence of Aβ plaques in the brains. At 9 months of age, Tg animals (one of three for 7-5 line and two of three for 7-9 line) began to exhibit a small number of Aβ plaques detectable in the hippocampus and entorhinal cortex. At 12, 15, 18 and 22 months of age, all of the Tg mice examined displayed considerable numbers of Aβ plaques (Fig. 4a, i). The hippocampus and entorhinal cortex were the sites most vulnerable to Aβ burden and the other cerebral cortices were moderately vulnerable. In animals with massive Aβ plaques, the molecular and granule cell layers of the cerebellum were also affected by Aβ deposition (not shown). The density of Aβ plaques increased as the animals aged in each of the Tg lines. Animals from the 7-5 line contain heavier density of Aβ plaques than those from the 7-9 line, when comparing animals of the same age. Non-transgenic littermates at 3–18 months of age showed no Aβ plaques throughout the brain.

T668-phosphorylated APP cytoplasmic domain accumulates in APP-SL Tg mice

The serial brain sections from APP-SL Tg mice aged at 3–22 months were immunostained by phosphorylation-independent Tau-5 and phosphorylation-dependent AT8 and PHF1. Plaques that were positively stained appeared in the animals aged at 12 months and over, and these tau-stained plaques constitute only a fraction of the Aβ plaques (Fig. 4l). A majority of the Aβ plaques were unlabeled by all of these tau antibodies (Fig. 4b). The tau labeling appeared as punctate granules located around Aβ plaques, and the tau-positive plaques were found in the entorhinal cortex and hippocampus, the most vulnerable sites to Aβ burden. The density of tau-positive plaques was prominently increased in the oldest animal examined. Immunostaining of the serial sections by anti-pT668 displayed results contrasting those obtained by the tau antibodies. All of the Aβ plaques detected in all the brain areas examined were positively labeled for anti-pT668 (Fig. 4c, j). The immunoreactive profile covered wider areas of Aβ plaques

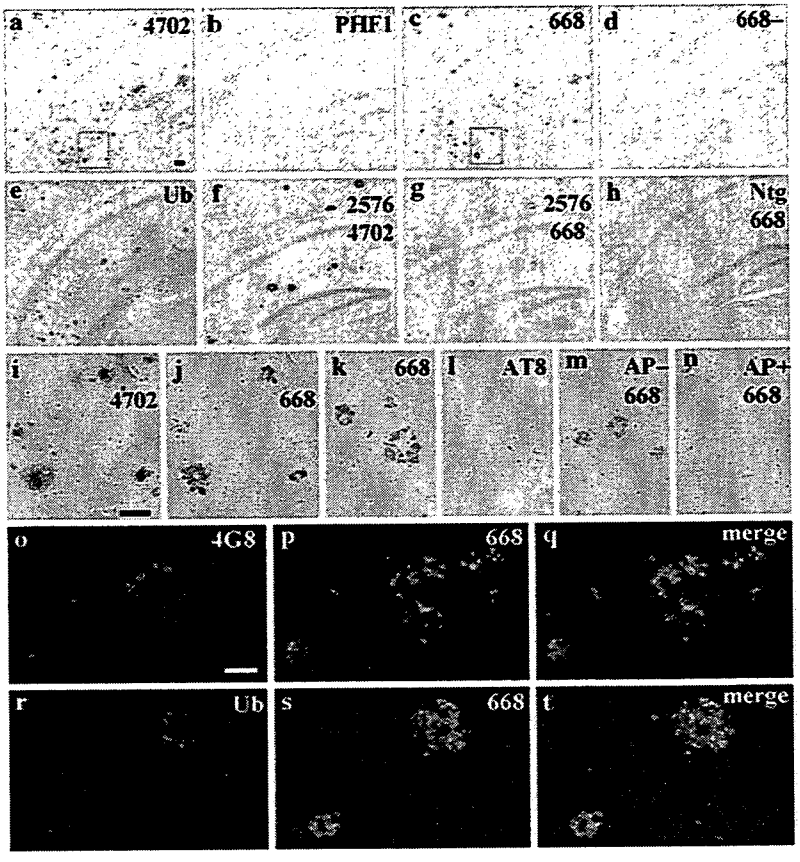

Fig. 4 Accumulation of pT668-ACD in dystrophic neurites of Aβ plaques formed in the brain from APP-SL Tg mouse. **a–e, i–n** Immunohistochemistry of serial brain sections from a 12-month-old APP-SL Tg 7-5 mouse using antibody to Aβ (4702) (**a, i**), PHF1 (**b**), anti-pT668 (668) (**c, j, k, m, n**), anti-ubiquitin (Ub) (**e**) and AT8 (**l**), or without primary antibody (**d**). **i** and **j** are higher magnification pictures of areas outlined by *squares* in a and c, respectively. The serial sections (**m, n**) were pretreated in parallel without (**m**) and with (**n**) alkaline phosphatase (*AP*). **f, g** Immunohistochemistry of serial brain sections from a 15-month-old Tg2576 (2576) mouse using 4702 (**f**) and anti-pT668 (**g**). **h** Immunohistochemistry of brain section from a 12-month-old non-transgenic mouse (Ntg) using anti-pT668. **o–t** Double immunofluorescence of the same APP-SL Tg 7-5 mouse brain sections using 4G8 (**o**) and anti-pT668 (**p**) with merged image (**q**) or using anti-ubiquitin (**r**) and anti-pT668 (**s**) with merged image (**t**). **a–h, i–n** and **o–t** are at the same magnifications, respectively. *Scale bars* 100 μM (**a, i**), 50 μM (**o**)

than the tau antibodies (Fig. 4k, l). At 9 months of age when Aβ plaques begin to emerge, all of these tau-negative Aβ plaques were positively stained for anti-pT668, indicating that accumulation of pT668-ACD occurs earlier than that of tau. Omission of anti-pT668 gave no immunoreaction, indicating its specificity (Fig. 4d). Treatment with alkaline phosphatase prior to immunostaining by anti-pT668 abolished the labeling of the Aβ plaques, confirming that T668 of APP cytoplasmic domain is phosphorylated (Fig. 4m, n). The anti-ubiquitin antibody also stained Aβ plaques with the similar immunoreactive profile as anti-pT668 (Fig. 4e), and the ubiquitin labeling was seen for all of the Aβ plaques. Therefore, a majority of Aβ plaques found in APP-SL Tg mice are positive both for pT668-ACD and ubiquitin, but negative for tau. These results indicate a possibility that pT668-ACD accumulating in Aβ plaques is ubiquitinated. The brains from Tg2576 mice aged 12 and 15 months were included to examine immunohistochemically by anti-pT668 for comparison. Aβ plaques developed in the Tg2576 mice were also positively immunostained using anti-pT668 and displayed similar immunoreactive profile and densities of the positively stained plaques as were seen for APP-SL Tg mice (Fig. 4f, g). Thus the accumulation of pT668-ACD in Aβ plaques is not unique to our APP-SL Tg mice, but might be a general finding common to Aβ plaques of mutant APP Tg mice. The non-transgenic littermates did not show plaque structures revealed by anti-pT668 throughout the brain (Fig. 4h). Double immunofluorescence of APP-SL Tg mice by 4G8 and anti-pT668 showed that accumulated Aβ and pT668-ACD appear mingled, but do not merge at all, indicating that Aβ and pT668-ACD are not colocalized (Fig. 4o–q). Double immunofluorescence by anti-ubiquitin and anti-pT668 revealed that ubiquitin and pT668-ACD are partly merged, indicating that pT668-ACD accumulated in the Aβ plaques is ubiquitinated (Fig. 4r–t). Thus, extracellular deposition of Aβ plaques is accompanied by intracellular accumulation of ubiquitinated pT668-ACD.